Neuro-Oncology
25(4), 674–686, 2023 | https://doi.org/10.1093/neuonc/noac212 | Advance Access date 2 September 2022

A distinct pattern of growth and RAC1 signaling in melanoma brain metastasis cells

Ioana Stejerean-Todoran, Phyllis A. Gimotty, Andrea Watters, Patricia Brafford, Clemens Krepler, Tetiana Godok, Haiyin Li, Zuriñe Bonilla del Rio, Anke Zieseniss, Dörthe M. Katschinski, Sinem M. Sertel, Silvio O. Rizzoli, Bradley Garman, Katherine L. Nathanson, Xiaowei Xu, Qing Chen, Jack H. Oswald, Michal Lotem, Gordon B. Mills, Michael A. Davies, Michael P. Schön, Ivan Bogeski, Meenhard Herlyn, and Adina Vultur

Department of Cardiovascular Physiology, Molecular Physiology, University Medical Center Göttingen, Göttingen, Germany (I.S.-T., Z.B.D.R., I.B., A.V.); Department of Biostatistics, Informatics and Epidemiology, University of Pennsylvania School of Medicine, Philadelphia, Pennsylvania, USA (P.A.G.); Program of Cellular and Molecular Oncogenesis, Melanoma Research Center, The Wistar Institute, Philadelphia, Pennsylvania, USA (A.W., P.B., C.K., T.G., H.L., M.H., A.V.); Department of Cardiovascular Physiology, University Medical Center Göttingen, Göttingen, Germany (A.Z., D.M.K.); Department of Neuro- and Sensory Physiology, University Medical Center Göttingen, Göttingen, Germany (S.M.S., S.O.R.); Department of Medicine, Division of Translational Medicine and Human Genetics; Abramson Cancer Center; University of Pennsylvania Perelman School of Medicine, Philadelphia, Pennsylvania, USA (B.G., K.L.N.); Department of Pathology and Laboratory Medicine, University of Pennsylvania, Philadelphia, Pennsylvania, USA (X.X.); Immunology Microenvironment and Metastasis, The Wistar Institute, Philadelphia, Pennsylvania, USA (Q.C., J.H.O.); Sharett Institute of Oncology, Hadassah Hebrew University Medical Center, Jerusalem, Israel (M.L.); Department of Melanoma Medical Oncology, MD Anderson Cancer Center, University of Texas, Houston, Texas, USA (G.B.M., M.A.D.); Department of Dermatology, Venereology and Allergology, University Medical Center Göttingen, Göttingen, Germany (M.P.S)

Corresponding Authors: Meenhard Herlyn, D.V.M., D.Sc., Program of Cellular and Molecular Oncogenesis, Melanoma Research Center, The Wistar Institute, Philadelphia, PA, USA (herlynm@wistar.org); Adina Vultur, Ph.D., The Wistar Institute, 3601 Spruce Street, Philadelphia, PA, 19104, USA (adinavultur1@gmail.com).

Abstract

Background. Melanoma, the deadliest of skin cancers, has a high propensity to form brain metastases that are associated with a markedly worsened prognosis. In spite of recent therapeutic advances, melanoma brain lesions remain a clinical challenge, biomarkers predicting brain dissemination are not clear and differences with other metastatic sites are poorly understood.

Methods. We examined a genetically diverse panel of human-derived melanoma brain metastasis (MBM) and extracranial cell lines using targeted sequencing, a Reverse Phase Protein Array, protein expression analyses, and functional studies *in vitro* and *in vivo*.

Results. Brain-specific genetic alterations were not detected; however, MBM cells *in vitro* displayed lower proliferation rates and MBM-specific protein expression patterns associated with proliferation, DNA damage, adhesion, and migration. MBM lines displayed higher levels of RAC1 expression, involving a distinct RAC1-PAK1-JNK1 signaling network. RAC1 knockdown or treatment with small molecule inhibitors contributed to a less aggressive MBM phenotype *in vitro*, while RAC1 knockdown *in vivo* led to reduced tumor volumes and delayed tumor appearance. Proliferation, adhesion, and migration were higher in MBM vs nonMBM lines in the presence of insulin or brain-derived factors and were affected by RAC1 levels.

Conclusions. Our findings indicate that despite their genetic variability, MBM engage specific molecular processes such as RAC1 signaling to adapt to the brain microenvironment and this can be used for the molecular characterization and treatment of brain metastases.

Key points

- Genetically diverse brain-derived melanoma cells display slow growth and high RAC1 expression.
- RAC1/PAK1/JNK1 signaling is active in melanoma brain metastasis cells and can be targeted with inhibitors.
- Insulin and brain-derived factors stimulate RAC1 signaling and aggressive melanoma brain cell phenotypes.

Graphical Abstract

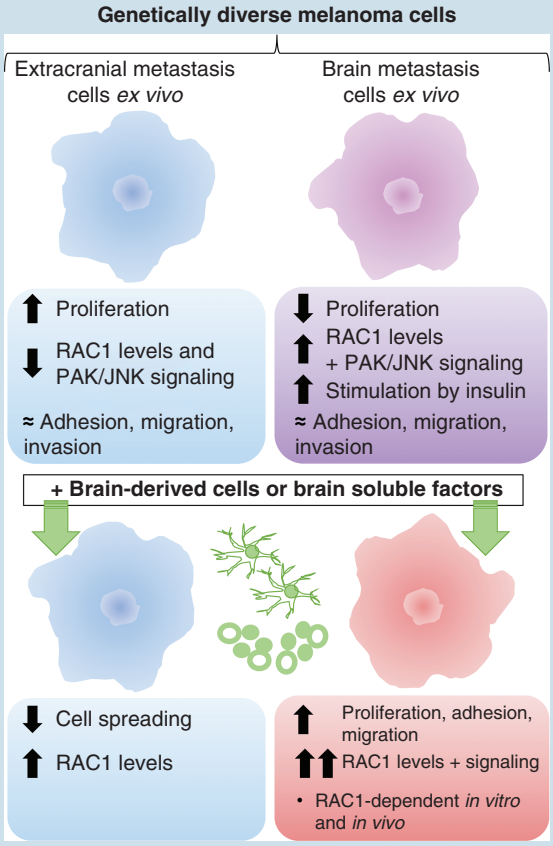

Importance of the Study

Brain metastasis is a deadly complication for cancer patients and remains poorly treated and understood. Our work shows that genetically diverse melanoma brain metastasis cells can acquire higher RAC1 levels and signaling while also displaying a slower proliferation rate compared to extracranial melanoma cells, thus unique brain-derived pathobiological properties. RAC1 confers a growth advantage to melanoma brain metastasis cells *in vitro* and *in vivo* and can be targeted therapeutically. While RAC1 mutations are known drivers of melanoma, our study suggests that RAC1 expression levels should also be considered to assess aggressive tumor behavior. Additionally, brain-derived melanoma cells respond more favorably to insulin and brain-derived factors; therefore, brain metastases studies are best conducted in the presence of brain-like environments.

Brain metastases constitute some of the most lethal complications in melanoma, occurring in over 50% of patients with metastatic disease.[1] Current therapeutic approaches against systemic melanoma include immunotherapy, targeted therapy, or combination treatments; brain lesions add surgery and radiotherapy to the list.[2,3] Although modern treatments have shown activity in the brain, there remains a high risk of mortality and resistance compared to extracranial lesions.[1,2,4,5] Multiple factors can contribute to brain metastasis therapy resistance including the blood-brain barrier,

genetic and immunological heterogeneity, also the brain microenvironment.[4,6] However, our understanding of melanoma brain metastasis (MBM) is limited and new disease models are needed for this purpose.[7]

Hypotheses posit that brain metastases result from the seeding of circulating tumor cells in the brain microvasculature, where they colonize following adaptation.[2] The strong influence of the brain microenvironment was shown when human cancer cells were xenografted into different organs in mice and analyses revealed complete gene expression reprogramming, and even gain of neuronal characteristics.[8] Given that melanocytes are derived from the neural crest, it is conceivable that they acquire and benefit from molecular mechanisms supported by the brain.[9] Early studies demonstrated that cells isolated from mouse MBM displayed arrest or death and enhanced migration in the presence of mouse brain soluble factors, while cutaneous-based melanoma cells behaved differently, suggesting unique biological responses intrinsic to MBM.[10]

Brain tissue is structurally and metabolically distinct, it also harbors neurons, microglia, and astrocytes, which can contribute to MBM biology directly or through secreted factors.[11,12] One study showed that astrocytes activate the proliferator-activated receptor γ pathway in MBM, exerting a prometastatic effect.[13] Analyses using patient-matched brain and extracranial metastases also identified immunosuppression and oxidative phosphorylation enrichment in MBM.[4,14] Altogether, increasing studies reveal intrinsic and extrinsic signals contributing to MBM-unique properties. *In vivo* studies using patient-derived xenografts (PDX) meanwhile, showed that human MBM-derived cells can cause mouse brain lesions starting from a subcutaneous injection, but this potential is uncertain after long-term *in vitro* culture, reaffirming the importance of the brain microenvironment in maintaining MBM properties.[7,15]

Currently, few studies demonstrate the presence of brain-specific genetic alterations in MBM; however, insights are emerging.[16,17] For example, RAS mutations and genetic alterations associated with sensitivity to PI3K/AKT/mTOR, cyclin-dependent kinases, and epidermal growth factor receptor (EGFR) inhibitors were highlighted.[18–20] PI3K pathway inhibitors in particular showed efficacy in preclinical MBM models and this pathway is one of the most frequently activated in MBM.[12,18,21,22] PI3K signaling can increase through mutations of its effectors (e.g. $AKT1^{E17K}$), by upstream activators (e.g. RAS), or through regulator loss (e.g. the phosphatase and tensin homolog [PTEN]).[20,23] However, the MBM molecular targets mentioned so far are by no means comprehensive.[24]

Here, we characterized a new panel of genetically diverse human-derived MBM cell lines, investigated new brain-specific biological processes, and we explored anti-MBM therapeutic approaches. To do so, we used genetic and protein analyses, functional studies in standard 2-dimensional (2D) and 3-dimensional (3D) cultures, and *in vivo* observations.

Materials and Methods

Cell Culture and Reagents

The human MBM cell lines M230, M331, M450, WM4237, WM4265-2, and the nonMBM lines WM793, 1205Lu, WM983B, and WM3918 were established by our group and that of Dr. M. Lotem (Hadassah Medical Center, Israel); patient samples were collected under Institutional Review Board approval and were confirmed as melanomas (Supplementary Figure 1A).[15,25] Human astrocytes (ScienCell #1800, Carlsbad, USA) were a gift from Dr. C. Berndt. Reagents were purchased from Tocris Bioscience (Bristol, United Kingdom), Sigma-Aldrich (Munich, Germany), or Selleckchem (Houston, USA). Details in Supplementary Information.

Genetic Analyses

Melanoma cell lines were genetically characterized using a custom-targeted massively parallel sequencing panel consisting of 109 melanomagenesis-relevant genes (Supplementary Table 1). Detailed methods, analysis, mutation, and copy number calling were performed as previously described.[25]

Proliferation and Viability Assays

Proliferation and viability were assessed by manual cell counting using a Neubauer hemocytometer, by the CellTiter-Blue Cell Viability Assay (Promega, Mannheim, Germany), or by cell staining with crystal violet then imaging. Details in Supplementary Information.

Adhesion, Migration, and Invasion Assays

Adhesion was assessed by serum deprivation, short-term cell incubation and washing, and 4 hours recovery of remaining cells prior to CellTiter-Blue addition and measurement. For migration, cells in serum-free media were seeded in transwell inserts (Corning, New York, USA) and were allowed to migrate 24 hours towards preconditioned media with 10% FBS, neurobasal media, or human astrocyte media, prior to Hoechst staining and imaging. Invasion was measured similarly, with Matrigel (Corning) precoated inserts. Melanoma spheroids were generated over 96 hours and were evaluated with the Live/Dead Viability/Cytotoxicity Kit (Invitrogen, Carlsbad, USA). Details are available in Supplementary Information.

Reverse Phase Protein Array (RPPA)

Reverse Phase Protein Array (RPPA) and data processing were performed by the MD Anderson Center RPPA Core Facility (Houston, USA). Briefly, cell lysates (and controls) were printed on nitrocellulose-coated slides using a 2470-Microarray printer (Aushon Biosystems, Billerica, USA). Slides were probed with primary antibodies plus biotin-conjugated secondary antibodies followed by signal detection. Data were normalized using median-centering across antibodies.[26] RStudio (Boston, USA) was used for data visualization.

Western Blots (WB)

Protein extraction was performed using a Triton-based Lysis Buffer, then 25–100 μg of protein/sample were

resolved on 10% SDS-polyacrylamide gels. A Trans-Blot Turbo Transfer System (Bio-Rad, Hercules, USA) was used to transfer proteins to nitrocellulose membranes. Membranes were blocked with 5% BSA, incubated with primary antibodies overnight, then 1 hour with secondary antibodies (antibodies listed in Supplementary Table 2). WB was imaged and analyzed using an Odyssey Infrared Imaging System and Image StudioLite software (LI-COR, Lincoln, USA). Details are available in Supplementary Information.

Immunohistochemistry (IHC) and immunofluorescence (IF) assays

Human melanoma brain tumor specimens were collected and used under the Abramson Cancer Center's melanoma research program tissue collection protocol UPCC08607 in accordance with the IRB of the University of Pennsylvania. IHC was performed on 5-μm-thick, formalin-fixed, paraffin-embedded sections. A 3,3′-diaminobenzidine-peroxidase substrate system produced the brown-staining product. Mouse brain specimens containing GFP-tagged WM4265-2 MBM cells were generated via intracardiac injection.[13] IF was performed on 60-μm-thick whole mount sections and images were acquired with a LeicaSP5 confocal microscope. Antibodies are in Supplementary Table 2.

GTPase Activity Assays

RAC1 activity was measured using an Active RAC1 Pull-Down and Detection Kit (Thermo Fisher Scientific, Schwerte, Germany) according to the manufacturer's instructions. RhoA activity was measured using a similar pull-down assay; details in Supplementary Information.

Melanoma/Primary Hippocampal Neuron Coculture

Primary hippocampal cultures were prepared from P0 Wistar rats.[27] Melanoma cells were prestained with CellTracker-Green-CMFDA (Molecular Probes #C2925, Eugene, USA). Cocultures were imaged (Cytation5, BioTek) and analyzed with Matlab (Mathworks). The melanoma Circularity Score = Cell Perimeter^2/(4xπxarea), where, a perfect circle = 1. The Mann-Whitney U test was applied as a statistical test. Details in Supplementary Information.

Knockdown and Expression Experiments

Stable RAC1 downregulation was performed by shRNA transfection into melanoma cells with a lentiviral vector (pLKO.1). Lentiviral production was performed in HEK293TN (#LV900A-1-GVO-SBI, Heidelberg, Germany) over 48 hours and melanoma cell infection occurred 24 hours prior to puromycin selection. MISSION shRNAs were purchased from Sigma; Supplementary Table 3. NADPH oxidase (NOX) expression studies are in Supplementary Information and Supplementary Table 4.

In Vivo Studies

Experiments were performed in accordance with The Wistar IACUC protocol 201227 in NOD/LtSscidIL2Rγnull mice (NSG). The WM4237 MBM model was previously described.[7,15] Female and male mice (randomized) were implanted s.c. with 80 000 cells embedded in reduced growth factor BD-Matrigel Basement Membrane Matrix (Becton Dickinson, Bedford, USA); tumors were measured every 3–5 days. Details are available in Supplementary Information.

Statistical Analyses

Two-sample *t*-tests (2-sided, alpha = 0.05) evaluated differences between nonMBM and MBM cells, and compared control and shRAC1 groups. RPPA proteins were identified where the FDR associated with the *t*-test comparing protein expression of nonMBM and MBM cells was less than 0.05 or 0.1. A nested analysis of variance (ANOVA) was used to evaluate the difference between nonMBM and MBM cells when there were multiple independent experiments for each cell line. An ANOVA test was used for more than 2 groups; Tukey's procedure for pairwise comparisons; Dunnett's procedure to compare all groups to controls. A Wilcoxon rank sum test was used to compare the number of days to measurable tumors. With evidence of unequal variances, Welch's t-test or ANOVA was used. Details in Supplementary Information.

Results

Melanoma Brain Metastasis Cells Display Slow Proliferation and Distinct Signaling Patterns *In Vitro*

We generated human-derived melanoma cell lines from different patients and metastatic sites including brain lesions.[15,25] Targeted sequencing of these lines featured common melanoma-altered genes (Supplementary Table 1) and a cell line panel was selected to compare genetically diverse intracranial and extracranial melanoma cells (featuring mutant *BRAF*, mutant *N-RAS*, PTEN, NF1 loss). We observed no unique genetic patterns specific to our brain-derived lines (Table 1). Although the genetics of the melanoma cells varied, in standard culture our MBM cell lines displayed significantly reduced proliferation compared to nonMBM lines, shown by cell number (Figure 1A) and proliferation rate (Figure 1B). We also examined metastasis-associated properties, but MBM cells did not display significantly altered adhesion (Figure 1C, $P = .440$), migration (Figure 1D, $P = .425$), invasion (Figure 1E, $P = .630$), or spheroid collagen invasion (Figure 1F) compared to extracranial cells (statistics, Supplementary Table 5). Our observations indicated that genetically diverse MBM cells display reduced growth in standard cell culture but adhesive or invasive properties are similar to nonMBM cells.

We next investigated signaling pathways that could be uniquely activated in MBM. This was initiated by interrogating MAPK, PI3K, STAT3, and PD-L1 pathways.[20,28–30]

Table 1 Melanoma Cell Lines Established from Extracranial or Intracranial Lesions and Their Genetic Profile. Cell lines were selected to include wild type or mutant BRAF, wild type or mutant N-RAS, wild type or mutated PTEN, and NF1 loss in at least 2 lines.

Cell Line	Lesion Type	BRAF Status	N-RAS Status	Additional Gene Mutations	High Gain Copy Number	Homozygous Copy Loss
WM793	Vertical growth phase melanoma	V600E	Wild type	CDK4, EGFR, MAP3K5, PTEN, TERT	BRAF, CDK6, DYNC1I1, EGFR, EZH2, GNAS, MET, RAC1, SMO, SRC, TRRAP	
1205Lu	Lung metastasis	V600E	Wild type	CDK4, GRM3, MAP3K5, PREX2, PTEN, TERT	KRAS, MYC, NF1, RAC1, SNX31	CDKN2A/B
WM3918	Metastatic lesion	Wild type	Wild type	DCC, DYNC1I1, GRIN2A, KDR, PDGFRA, PREX2, PTPRD, PP6C, SOX10, TERT	MYC	CDKN2A, NF1
WM983B	Inguinal node metastasis	V600E	Wild type	ATM, CDKN2A, KDR, TERT, TP53	BRAF, EGFR, EZH2, MITF, RAC1	MMP8
M230	Brain metastasis	V600K	Q61R	GRM3, PTCH1, SETD2, TERT, TRRAP	AKT3, MDM4, MITF, MMP8, STK19, TERT	CDKN2A/B
M331	Brain metastasis	V600E	Wild type	ALK, BRCA2, CDKN2A, DDX3X, JAK3, MAP2K1, MAP3K9, PREX2, RB1, RET, RHOT1, STK11, TERT, TP53, TRRAP	STK19	NF1
M450	Brain metastasis	Wild type	Wild type	BAP1, CDKN2A, CTNNB1, DCC, DDX3X, FGFR3, GRIN2A, GRM3, MAP3K9, NF1, PTEN, PTPRK, ROS1, TP53, TRRAP, WT1		TP53
WM4237	Brain metastasis	V600E	Wild type	ATM, MET, PDGFRA, RB1, TERT, TP53,	BRAF, CDK6, DYNC1I1, EIF2AK3, EZH2, GRM3, MET,	
WM4265-2	Brain metastasis	Wild type	Q61K	ARID1B, CDKN2A, EGFR, NF1, PDGFRB, PTEN, TERT, TP53, TRRAP	MITF, STK19	

The most notable observation, also reported by others, was the activation of AKT (but not predicted by PTEN levels; Supplementary Figure 1B, C). To further examine brain-specific signaling, we used RPPA to determine the expression of 297 proteins in our cell line panel (Supplementary File 1). Proteins differentially expressed between MBM and nonMBM groups using a false discovery rate (FDR) of 0.05 were: 4E-BP1, TP53BP1, androgen receptor (AR), D-alpha tubulin, EGFR [pY1173], N-RAS, poly-(ADP-ribose) polymer (PAR), and TFRC (coefficient of variation, Supplementary Table 5). With the FDR of 0.1, we identified c-Abl, NF-κBp65 [pS536], PLCG2 [pY759], PREX1, and RICTOR. Categorizing these hits and including associated proteins differentially expressed in MBM, we observed expression differences related to PI3K/mTOR, N-RAS, and NF-κB signaling in our MBM lines (Figure 1G); these are linked signaling-wise (Supplementary Figure 1D). Distinct expression patterns were also found in migration/adhesion (Figure 1H) and DNA damage-related proteins (Figure 1I).

The importance of PI3K/AKT signaling in MBM has been demonstrated by multiple groups.[20] The involvement of RAS was also reported.[19] Meanwhile, the expression of mTOR and NF-κB effectors (Supplementary Figures 1E, F) was inconsistent. However, we observed a potential link with ras-related C3 botulinum toxin substrate 1 (RAC1) and this has not been extensively studied in MBM despite ras-related C3 botulinum toxin substrate 1 (RAC1) being among the top ten functionally mutated proteins in melanoma.[31] RAC1 is involved in PI3K and RAS signaling, it controls phosphorylation of the myosin-II heavy-chain and actinomyosin disassembly, as well as DNA damage.[32,33] PREX1 is a RAC1 guanine nucleotide exchange factor (GEF) and Merlin (low in MBM) is a tumor suppressor involved in RAC1-PAK1 signaling.[34] We, therefore, focused on further investigating the role of RAC1 in MBM.

MBM Cells Express High RAC1 Protein Levels

To examine the involvement of RAC1 in MBM, we explored RAC1 and Cdc42 expression in our panel of cell lines. We consistently detected higher total RAC1 protein levels in all our MBM compared to nonMBM lines, but not Cdc42 (Figure 2A) or RAC3 (Supplementary Figure 2A). Since standard 2D culture conditions are not fully representative of *in vivo* conditions, we also interrogated 3-dimensional (3D) spheroids. Under these conditions, we still observed higher MBM RAC1 levels (Figure 2B). RAC1 activity, however, was not increased (Figure 2C). Confirming *in vitro* results, RAC1 was also found highly expressed in human MBM patient samples, but variability exists (Figure 2D).

RhoA is in a regulatory feedback loop with RAC1.[35] However, our analyses showed no consistent increase in RhoA levels or activity in MBM (Supplementary Figure 2B–C). The RAC1 effector p21-activated kinase 1/serine/threonine-protein kinase 1 (PAK1) and downstream effector c-Jun N-terminal kinase 1 (JNK1) on the other hand, showed higher activation in 2D and 3D MBM cultures (Figure 2E–F).[36,37] These findings suggested a potential RAC1/PAK1/JNK signaling axis at play in our MBM cells, which is of interest given the important role of PAKs in drug resistance and RAC/PAK/JNK signaling in neurons.[38,39] Using IF staining, we detected diffuse cytoplasmic RAC1 expression in our MBM cell lines in 2D and 3D cultures, similar to our patient samples (Supplementary Figure 2D–E). Together, our findings suggested that high RAC1 levels played a unique role in MBM.

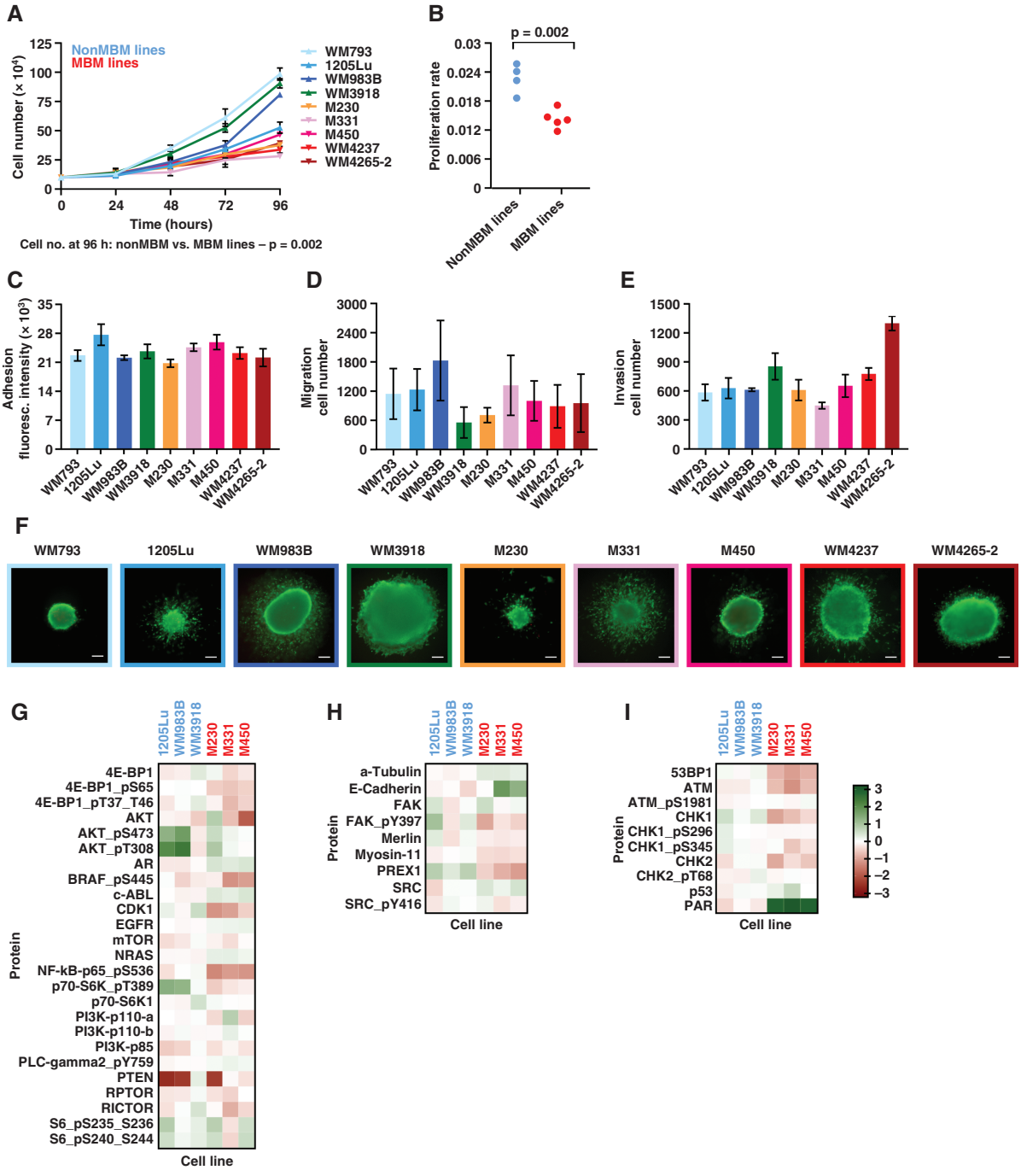

Fig. 1 **Melanoma Brain Metastasis Cells Display Distinct Proliferation and Signaling *In Vitro*.** (A) Proliferation of MBM (warm colors) vs nonMBM (cool colors) cells over 96 hours. Triangles represent the mean±SEM ($n = 12$ measurements; 4 wells/3 experiments/cell line). (B) Proliferation rates (estimated slopes) for MBM vs nonMBM cells. (C) Adhesion of MBM vs nonMBM cells. Data presented as mean±SEM ($n = 12$ as [A]). (D) Migration of MBM vs nonMBM cells over 24 hours. Data presented as mean±SEM ($n = 3$). (E) Invasion of MBM vs nonMBM cells through Matrigel (24 hours). Data presented as mean±SEM ($n = 3$). (F) Invasion of 3D melanoma spheroids through collagen (72 hours). Representative images ($n = 3$). Live cells (green); dead cells (red); scale bar: 100 μm. (A–E) Suppl.Table 5: statistics. (G–I) Heatmap generated from RPPA analyses featuring all hits with differential expression (FDR = 0.1); (G) proteins related to PI3K signaling, (H) migration/adhesion-related proteins, (I) DNA damage response elements.

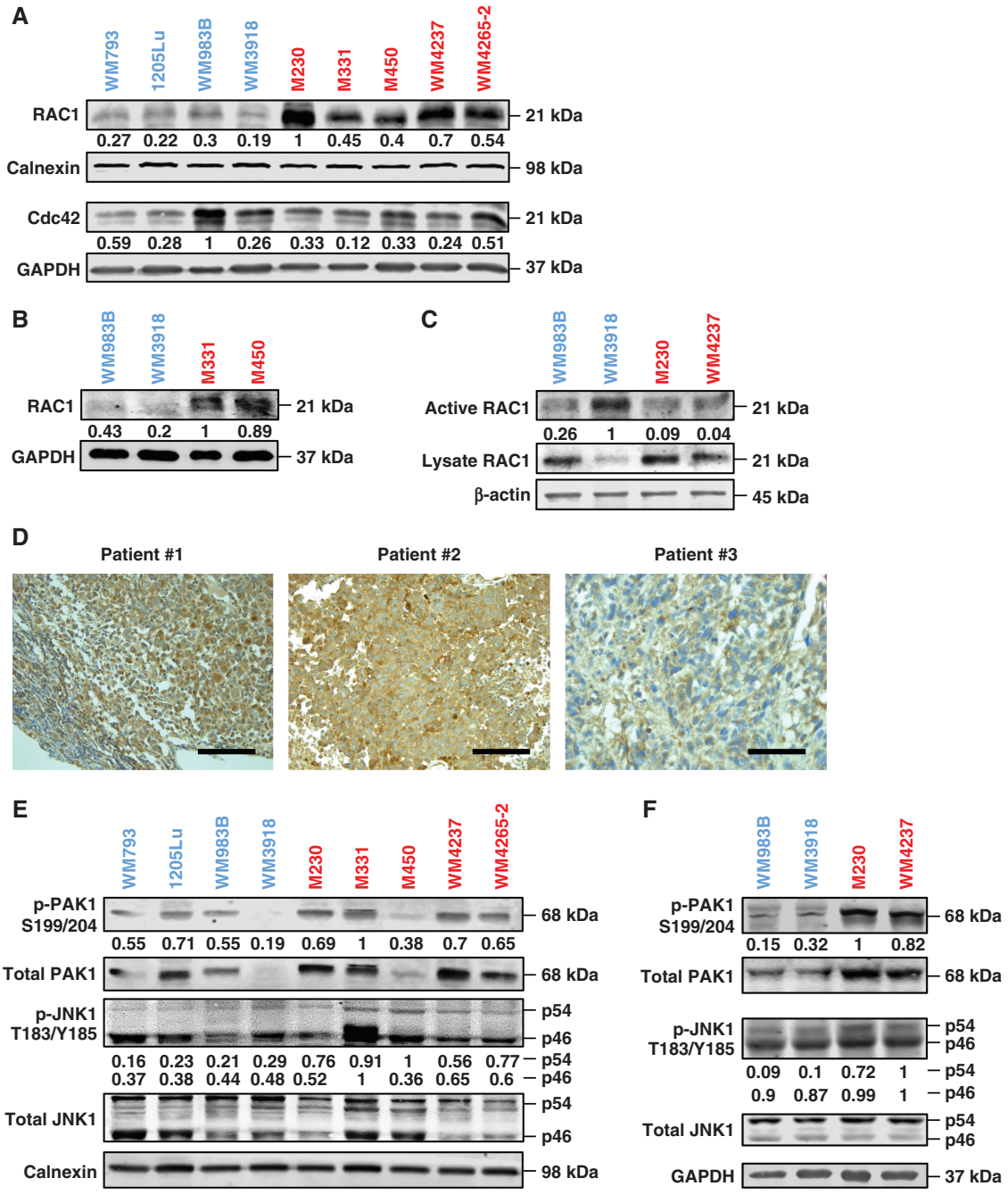

Fig. 2 **MBM Cells Express High RAC1 Protein Expression.** (A–C, E–F) NonMBM cell lines (blue); MBM cell lines (red). (A) WB analysis for RAC1 and Cdc42; band quantitation is the ratio between evaluated protein and controls (calnexin, GAPDH). (B) WB analysis of RAC1 in lysates from 3D collagen-embedded spheroids. Quantitation is the ratio between RAC1 and GAPDH. (C) Active RAC1 pull-down assay. Active RAC1 band quantitation is relative to total protein. Control: β-actin. (D) IHC staining of RAC1 (brown signal) in human melanoma brain tumor lesions ($n = 3$ patients). Scale bar: 100 μm. (E–F) WB analysis of PAK1 and JNK1 in (E) 2D lysates and (F) 3D lysates. Band quantitation is shown as the ratio between phosphorylated and total protein. Controls: calnexin, GAPDH.

RAC1 Inhibition Impairs Aggressive MBM Cell Phenotypes

Given previous reports of RAC1 GTPase-independent activity, we next investigated the importance of higher RAC1 levels in our MBM cell lines.[40] With shRNA knockdown (KD) of RAC1 (Supplementary Figure 3A), our melanoma cells had a slight reduction in proliferation, but this was not unique to MBM (Figure 3A, Supplementary Table 6). RAC1 KD also showed cell line-dependent effects on adhesion (Figure 3B), migration (Figure 3C), and invasion (Figure 3D–E). We next examined how RAC1-associated signaling

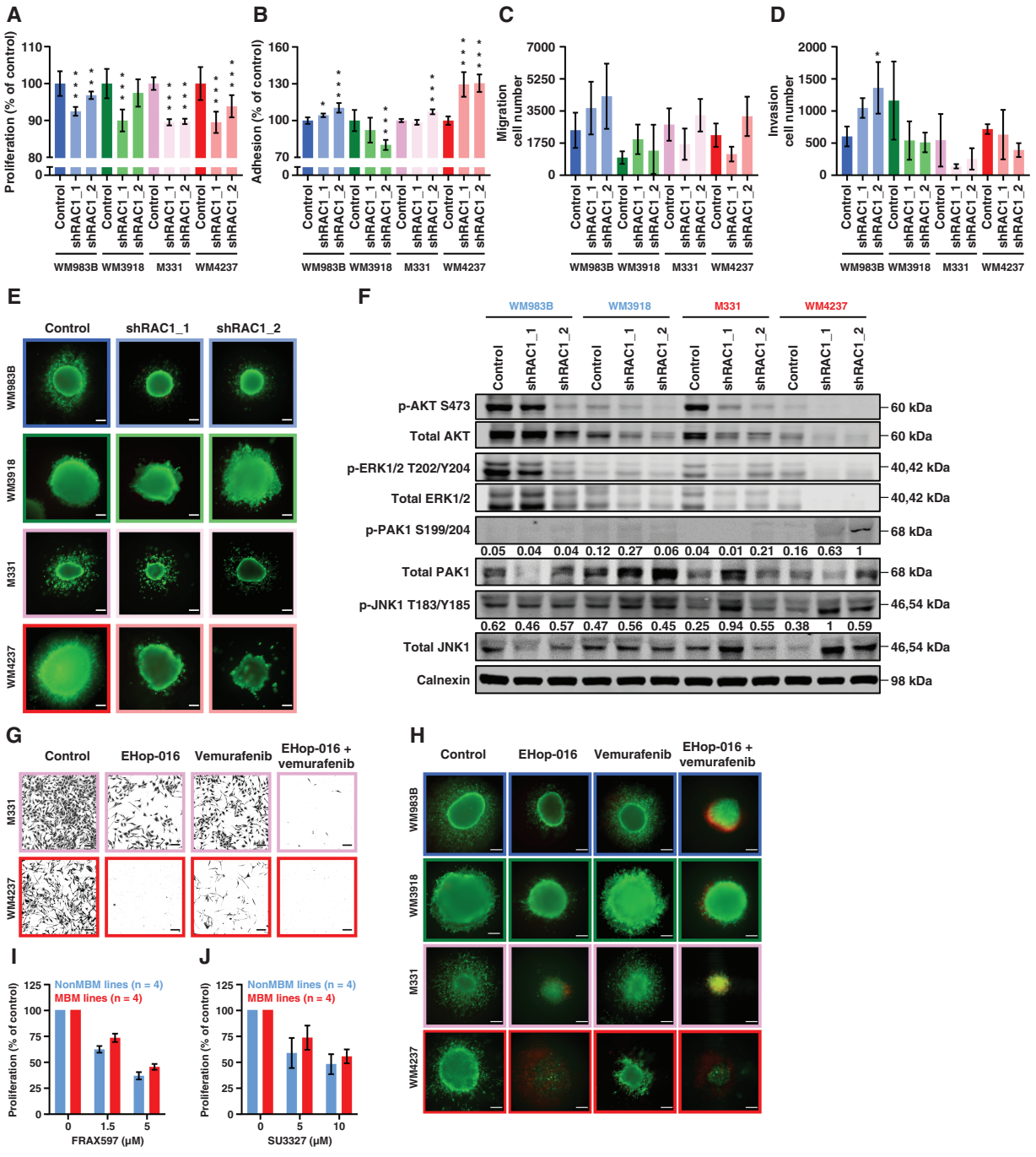

Fig. 3 **RAC1 Inhibition By Knockdown Or Targeted Inhibitors Impairs Aggressive MBM Phenotypes.** (A) Proliferation, (B) adhesion, (C) migration of MBM vs nonMBM cell lines with RAC1 KD over 72 hours. Data presented as mean±SEM (n = 12 measurements; 4 wells/3 experiments/condition). (D) Invasion of melanoma cells with RAC1 KD through Matrigel (24 hours). Data presented as mean±SEM (n = 12 as [A]). (E) Invasion of 3D spheroids through collagen (72 hours). Representative images (n = 3). Live cells (green), dead cells (red); scale bar: 100 μm. (F) WB analyses of adherent cells following RAC1 KD. Band quantitation is relative to total protein. Control: calnexin. (G) Inhibitors of RAC (EHop-016, 2.5 μM) and $BRAF^{V600E}$ (vemurafenib, 5 μM) in MBM cell culture over 72 hours. Representative images of crystal violet stained cells (n = 3). Scale bar: 50 μm. (Supplementary Figure 3B: quantitation). (H) Inhibitor treatment of 3D spheroids over 72 hours. Representative images (n = 3). Live cells (green), dead cells (red); scale bar: 100 μm. (Supplementary Figure 3C: quantitation). (I) Small molecule inhibitors targeting PAK and (J) JNK for 72 hours were assessed in MBM (M331, M450, WM4237, WM4265-2) and nonMBM cells (WM793, 1205Lu, WM983B, WM3918). Proliferation changes are shown as a mean of n = 4 cell lines/condition; each line contributed n = 4 wells/condition ±SEM from 3 experiments. (A–D, I–J) Supplementary Table 6: statistics; significance: $^{*}P \leq .05$, $^{**}P \leq .01$, $^{***}P \leq .001$.

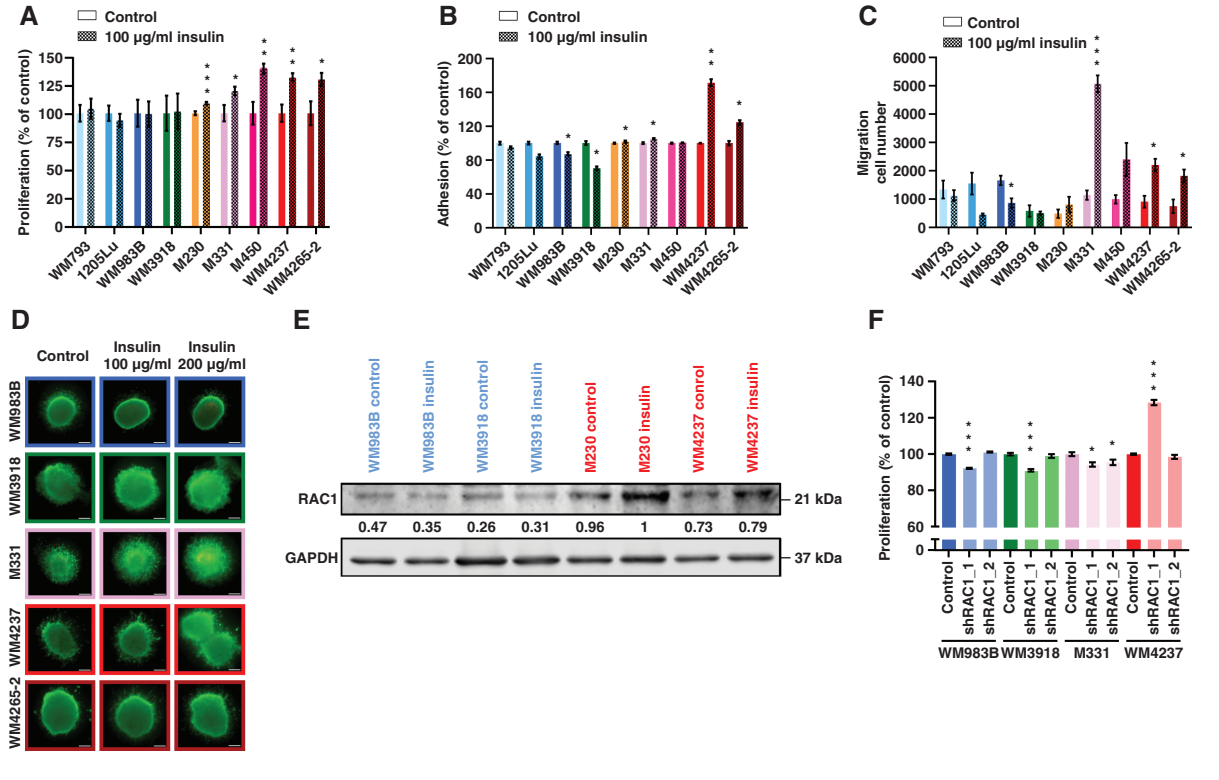

Fig. 4 Insulin Enhances MBM Growth, Adhesion, and Migration. (A) Proliferation, (B) adhesion, of MBM (warm colors) vs nonMBM (cool colors) cells following insulin treatment for 72 hours Data presented as mean±SEM ($n = 12$ measurements; 4 wells/3 experiments/cell line). (C) Migration of melanoma cells over 24 hours following 72 hours of insulin treatment. Data are presented as mean ± SEM ($n = 3$). (D) Invasion of 3D spheroids through collagen in the presence of insulin (72 hours). Representative images ($n \geq 4$). Live cells (green); dead cells (red); scale bar: 100 µm. (E) WB analysis of melanoma cells treated with insulin (100 µg/ml, 72 hours). RAC1 quantitation was normalized to the control GAPDH. (F) RAC1 KD melanoma cell proliferation in 100 µg/ml insulin (72 hours). Data presented as mean±SEM ($n = 12$ as [A]). Significance: $^{*}P \leq .05$, $^{**}P \leq .01$, $^{***}P \leq .001$. Supplementary Table 8: statistics.

was affected by its levels in standard culture. As Figure 3F shows, phosphorylated p-AKT and p-ERK levels were decreased in all lines. However, in MBM we observed higher p-PAK1 and p-JNK1, possibly to maintain signal activity (Figure 3F). These data further supported distinct RAC1/PAK1/JNK1 signaling in MBM but warranted more examination of the contribution of RAC1 to MBM.

The combination of $BRAF^{V600E}$ inhibitors with other targeted therapies showed positive clinical results.[41] We, therefore, tested vemurafenib with the RAC inhibitor EHop-016 against MBM cells and observed that this combination was more effective than either single agent (Figure 3G, Supplementary Figure 3B, and Supplementary Table 7). Similar effects were observed with 3D spheroids (Figure 3H, Supplementary Figure 3C, Supplementary Table 7). As a single agent, EHop-016 also inhibited melanoma proliferation and induced cell death (Supplementary Figure 3Di–ii; Supplementary Table 7), but the effects were strongest in combinations. Vemurafenib and the MEK inhibitor trametinib as single agents had only partial inhibitory effects on MBM cells (Supplementary Figure 3Ei–ii, Supplementary Table 7). Meanwhile, the PAK inhibitor FRAX597 (Figure 3I) and JNK inhibitor SU3327 (Figure 3J) both decreased cell proliferation, but FRAX597 required higher concentrations in MBM (Supplementary Table 7), possibly due to higher target levels or compensatory signaling. Summarized, our results showed that targeting RAC/PAK/JNK *in vitro* was effective against melanoma cells, including brain-derived cells, and combination therapies were most robust to eradicate MBM cells. These data also suggested a biological role for high RAC1 in MBM, especially since RAC1 can affect multiple functional mechanisms and pathways by binding to different molecular partners.

Insulin Enhances MBM Proliferation, Adhesion, Migration, and Invasion *In Vitro*

In standard culture, RAC1 function or reliance may not be fully engaged in MBM despite high protein levels being present. To understand the plasticity of MBM in different microenvironments, we stimulated MBM cells using insulin, IGF-1, VEGF, glucose, or cell density. Only human insulin significantly stimulated the proliferation of all MBM lines compared to extracranial lines (Figure 4A, Supplementary Figure 4A–D, and Supplementary Tables 89). Adhesion, migration, and invasion were also altered in MBM compared to nonMBM lines following insulin treatment (Figure 4B–D, Supplementary Figure 4E,

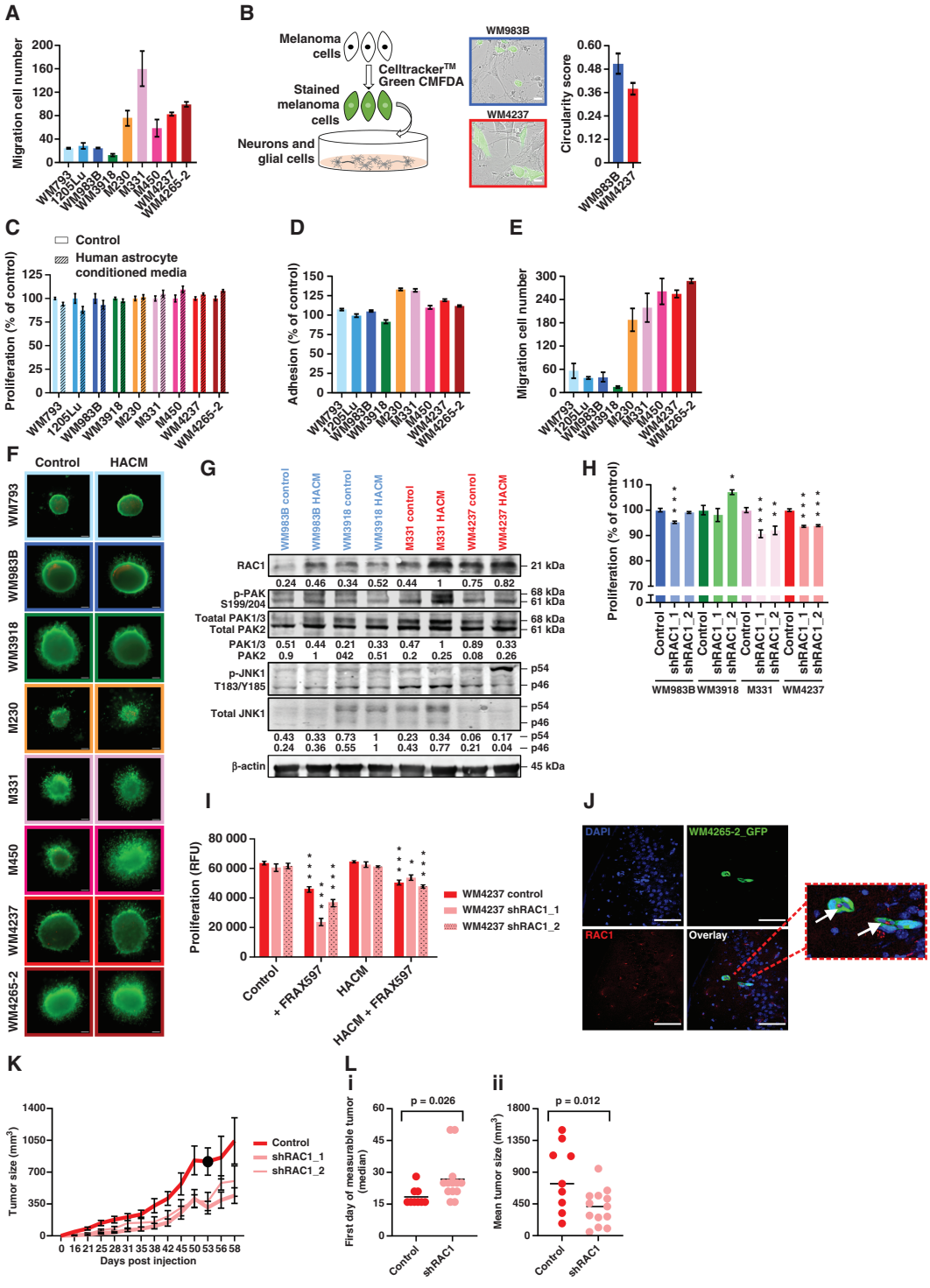

Fig. 5 **Brain-Associated Factors Enhance MBM Growth, Adhesion, Migration, and Invasion.** (A) Melanoma migration in conditioned media from rat glia and neuron cocultures. Data presented as mean±SEM ($n = 3$). (B) Melanoma cell spreading in rat glia and neuron cocultures (72 hours). Representative images ($n = 3$). Scale bar: 50 µm. Circularity score applies to melanoma cells only; a higher score = greater circularity. Data shown as mean±SEM (WM983B, $n = 32$; WM4237, $n = 82$). (C) Proliferation in HACM (72 hours). Data presented as mean±SEM ($n = 12$ from 4 wells/3 experiments/cell line). (D) Adhesion in HACM. Data presented as mean±SEM ($n = 12$ as [C]). (E) Migration (24 hours) in HACM. Data presented as mean±SEM ($n = 3$). (F) Invasion of 3D spheroids through collagen, with HACM (72 hours). Representative images ($n \geq 6$). Live cells (green); dead cells (red); scale bar: 100 µm. (A–F) Experimental schematics are available in Supplementary Figure 5. (G) WB analysis of melanoma cells in HACM (72 hours). RAC1 quantitation was normalized to β-actin; for PAK/JNK it is the ratio between phosphorylated and total protein. (H) Proliferation of

Supplementary Table 9). Additionally, insulin increased RAC1 protein expression (Figure 4E) while RAC1 KD dampened insulin-stimulated proliferation (Figure 4F, Supplementary Table 8). These MBM results parallel the important role of insulin for neuronal maintenance.[42]

Brain-Derived Factors Enhance MBM Aggressive Behavior *In Vitro* And *In Vivo*

The brain microenvironment could further stimulate MBM cells compared to nonMBM cells; therefore, we tested cell behavior in the presence of conditioned media from rat neurons and glia cocultures. Under these conditions, MBM cell migration was significantly higher compared to nonMBM migration ($P < .001$; Figure 5A, Supplementary Figure 5A). In addition, MBM cells grown among rat neural cells showed significant ($P < .001$) spreading (Figure 5B). Exposure of melanoma cells to human-derived astrocyte conditioned media (HACM) only increased proliferation in 2 out of 5 MBM lines (Figure 5C, Supplementary Figure 5B). However, most interesting was the significant difference in adhesion ($P < .001$; Figure 5D, Supplementary Figure 5C), migration ($P < .001$; Figure 5E, Supplementary Figure 5D), and invasion in the presence of HACM (Figure 5F, Supplementary Figure 5E–F, Supplementary Table 10). WB analyses showed that total-RAC1 and phosphorylated-PAK expression were also elevated under these conditions but not RAC1 activity (Figure 5G, Supplementary Figure 5G), suggesting the important role of the brain microenvironment in promoting RAC1/PAK signaling but not necessarily through higher GTP-RAC1. In the presence of RAC1 KD (Figure 5H) or FRAX597 (Figure 5I), proliferation was significantly decreased, even in the presence of HACM; decreases in adhesion and migration were also observed (Supplementary Figure 5H, I, and J, Supplementary Table 10). These data demonstrated the contribution of RAC1 to MBM in the presence of brain-derived factors.

An intracardiac-induced *in vivo* mouse model of human MBM showed single melanoma cells in the brain displaying focused RAC1 areas (Figure 5J); this is in contrast to the diffuse RAC1 signal observed in patient tumors and spheroids. Since single cells neighbor different cell types, RAC1 may have different functions and localization depending on the environment and proliferation status. To confirm that RAC1 levels are essential to MBM *in vivo*, we used a MBM-PDX model (WM4237) that recapitulates human disease, starting from a s.c. injection site and disseminating to the brain.[7,15] We injected WM4237 cells with RAC1 shRNA in NSG mice and monitored primary tumors and metastasis using a luciferase signal (Figure 5K). RAC1 KD significantly delayed tumor appearance (P-value = .026; Figure 5Li) and reduced tumor volumes (P-value = .012; Figure 5Lii). Due to aggressive primary disease in the control group following our *ex vivo* MBM handling, studies were halted prior to brain-lesion detection (data not shown); however, our findings still support the important role of RAC1 for MBM tumor latency and growth *in vivo*.

Because RAC1 regulates reactive oxygen species (ROS) generation, we also investigated if NOX mRNA levels were altered in MBM.[43] No unique NOX expression patterns were observed (Supplementary Figure 6A, Supplementary Information) and the response to redox-regulating agents was also nonspecific (Supplementary Figure 6B–C). While the role of ROS in MBM needs further exploration, our preliminary studies suggest this work, as well as further studies on RAC1 in MBM, could all benefit from more *in vivo*-like experimental conditions.

Discussion

In this study, we aimed to identify MBM-specific molecular processes with therapeutic potential. Our cell lines displayed no clear or unique genetic alterations using targeted sequencing analyses, in line with what is reported so far.[20] However, our MBM cell lines displayed slower proliferation rates *in vitro* and this was only enhanced by insulin or HACM. This observation suggests remnants of a dormant phenotype, stimulated by specific conditions.[2] Our MBM lines did not display higher adhesion, migration, or invasion potential *in vitro* compared to nonMBM lines, suggesting these functions are not selected for, or these properties are lost *ex vivo*. Brain-derived microenvironment factors, on the other hand, played an important role in further teasing-out MBM differences.

Regarding distinct signaling, analyses of melanoma brain specimens previously highlighted pathways such as INK4a-CDK4/6-RB, ARF-p53-MDM2, RAS-RAF-MAPK, and PTEN-PI3K-AKT, among others.[44] These pathways were also found upregulated in our MBM cells (by RPPA); however, we also detected RAC1 effectors, later validated by high RAC1 protein expression analyses. *Rac1* nonsilent mutations are found in approximately 5% of melanomas and the *RAC1*P29S mutation is the third most common hotspot mutation in melanoma.[31,45] Differences in RAC1 expression could therefore also contribute to aggressive cases.

RAC1 is a member of the Rho family of GTPases that regulates MAPK, mTOR, NF-κB signals, and multiple functions; it also plays a critical role in neuritogenesis and neuronal migration.[46] In our MBM lines, RAC1 appeared

Fig. 5 continued

RAC1 KD melanoma cells in HACM (72 hours). Data presented as mean±SEM ($n = 12$ as [C]). (I) Effects of FRAX597 (1.5μM-72hours) on shRAC1 KD cell proliferation in the presence of HACM. Comparisons focus on untreated vs FRAX597, and HACM vs HACM+FRAX597 treatments. Data presented as mean ± SEM ($n = 6$ from 2 wells/3 separate experiments/condition). (J) IF staining of whole mount slides featuring mouse brains with GFP-tagged WM4265-2 human MBM cells (representative images). The mouse MBM model was generated over 4 weeks following intracardiac injection. DAPI (blue), GFP (green), RAC1 (red). Scale bar: 100 μm. Inset: white arrows point to focused RAC1 signals within WM4265-2 cells. (K) *In vivo* tumor growth of WM4237 with RAC1 KD in NSG mice. A summary of tumor size per group is shown over 58 days; tumors were resected for 2 mice in the control group (day 53, black dot). Control ($n = 9$), shRAC1_1 ($n = 9$), shRAC1_2 ($n = 4$). (L) (i) Median time to first measurable tumor (days); (ii) mean tumor size with or without RAC1 KD on day 50. Significance: $^{*}P \leq .05$, $^{**}P \leq .01$, $^{***}P \leq .001$. Supplementary Table 8: statistics.

associated with PAK1/JNK1 signaling and to be stimulated by brain-derived factors. PAK1 is important for neuronal polarization and differentiation, while JNKs regulate cell death in the nervous system.[47,48] Therefore, there could be a brain-induced reprogramming of metastasized melanoma cells featuring a gain of neuronal characteristics. Interestingly, RPPA analyses conducted on other tumor types also reveal PAK1 and JNK as differentially expressed in brain samples.[49]

Our observed increase in RAC1 levels in MBM without higher activity *in vitro* does not dismiss its important role.[40] Cells could be poised for activation in brain-like environments, a possibility given that we could stimulate MBM proliferation, invasion, and RAC1 expression with insulin or brain-derived factors. Interestingly, insulin is needed for neuronal survival, circuitry, and synaptic activity.[50] Additionally, RAC1 KD affected MBM growth and latency *in vivo*. The WM4237 MBM model requires long periods (>17 weeks) for brain metastasis detection.[7] This study was the first attempt to use this model for biological studies and our results suggest that it is best used with limited *ex vivo* cell handling.

With respect to drug resistance, we observed partial response of our MBM cells to BRAF/MEK inhibitors, but combination approaches including a RAC inhibitor that eradicated almost all MBM cells, and PAK and JNK inhibitors were also effective, indicating the potential of co-targeting MBM-specific pathways to achieve a greater anti-MBM response.

We acknowledge that many of our findings are *in vitro* and could apply to only a subset of patients with MBM; nevertheless, our first attempt at characterizing a diverse panel of MBM cell lines unraveled unique properties. In sum, our findings highlight the importance of RAC1 signaling for MBM and the need to recapitulate the brain microenvironment for MBM-based studies.

Supplementary Material

Supplementary material is available online at *Neuro-Oncology* (http://neuro-oncology.oxfordjournals.org/).

Keywords

brain | melanoma | metastasis | microenvironment | RAC1

Funding

Work supported by: the National Cancer Institute (NCI, PO1-CA114046, P01-CA025874, P30-CA010815, and R01-CA047159), the Dr. Miriam and Sheldon G. Adelson Medical Research Foundation to M.H.; the German Research Foundation (DFG, SFB1027-C4, SFB1190-P17, BO3643/3-2, and IRTG1816) to I.B.; the American Cancer Society (ACS-IRG-96-153-10) to A.V.; NCI (R01-CA241490) to Q.C. The Wistar Institute core facilities are funded by the Cancer Center Support Grant P30-CA010815.

Acknowledgments

We thank Carsten Berndt (Heinrich-Heine University Düsseldorf, Germany) for human astrocytes and Paul Lieberman (The Wistar Institute, USA) for the pCDH-EF1a-eFFly-mCherry plasmid. We thank Andrea Paluschkiwitz, Christine Gibhardt, Xin Zhang, Sabine Krull, Annette Bennemann, Min Xiao, Haiwei Mou, Angela Boshnakovska, Christina Zeissing, Russell Ney, Ashani Weeraratna, and The Wistar Institute's Imaging and Flow Cytometry Facilities for their expert assistance.

Conflict of Interest

The authors declare no potential conflicts of interest.

Authors' Contribution

Conceptualization: A.V., I.S.-T., M.H. Experimentation: I.S.-T., A.V., A.W., P.B., C.K., T.G., H.L., Z.BdR., A.Z., S.M.S., B.G., S.S., A.Z., X.X., Q.C., J.H.O. Writing: A.V., I.S.-T. Resources: I.B., M.H., K.L.N., S.O.R., D.M.K., M.S., M.L., G.B.M., M.A.D., M.P.S. Analysis: I.S.-T., P.A.G., A.V., P.B., B.G., K.L.N., G.B.M., M.A.D. Supervision: A.V., I.B., M.H.; Funding: I.B., M.H., A.V. Proofreading: all authors.

References

1. Glitza Oliva I, Tawbi H, Davies MA. Melanoma brain metastases: current areas of investigation and future directions. *Cancer J.* 2017;23(1):68–74.
2. Achrol AS, Rennert RC, Anders C, et al. Brain metastases. *Nat Rev Dis Primers.* 2019;5(1):1–26.
3. Dummer R, Ascierto PA, Nathan P, Robert C, Schadendorf D. Rationale for immune checkpoint inhibitors plus targeted therapy in metastatic melanoma: a review. *JAMA Oncol.* 2020;6(12):1957–1966.
4. Fischer GM, Jalali A, Kircher DA, et al. Molecular profiling reveals unique immune and metabolic features of melanoma brain metastases. *Cancer Discov.* 2019;9(5):628–645.
5. Lamba N, Aizer AA. The evolving role of systemic therapy and local, brain-directed treatment in patients with melanoma and brain metastases. *Neuro Oncol.* 2021;23(11):1816–1817.
6. Han CH, Brastianos PK. Genetic characterization of brain metastases in the era of targeted therapy. *Front Oncol.* 2017;7:1–11.
7. Valiente M, Van Swearingen AED, Anders CK, et al. Brain metastasis cell lines panel: a public resource of organotropic cell lines. *Cancer Res.* 2020;80(20):4314–4323.
8. Park ES, Kim SJ, Kim SW, et al. Cross-species hybridization of microarrays for studying tumor transcriptome of brain metastasis. *Proc Natl Acad Sci USA.* 2011;108(42):17456–17461.
9. Kasemeier-Kulesa JC, Romine MH, Morrison JA, et al. NGF reprograms metastatic melanoma to a bipotent glial-melanocyte neural crest-like precursor. *Biol Open.* 2018;7(1):1–11.

10. Klein A, Sagi-Assif O, Izraely S, et al. The metastatic microenvironment: Brain-derived soluble factors alter the malignant phenotype of cutaneous and brain-metastasizing melanoma cells. *Int J Cancer.* 2012;131(11):2509–2518.
11. Quail DF, Joyce JA. The microenvironmental landscape of brain tumors. *Cancer Cell.* 2017;31(3):326–341.
12. Phadke M, Ozgun A, Eroglu Z, Smalley KSM. Melanoma brain metastases: Biological basis and novel therapeutic strategies. *Exp Dermatol.* 2021;31:31–42.
13. Zou Y, Watters A, Cheng N, et al. Polyunsaturated fatty acids from astrocytes activate ppargamma signaling in cancer cells to promote brain metastasis. *Cancer Discov.* 2019;9(12):1720–1735.
14. Fischer GM, Guerrieri RA, Hu Q, et al. Clinical, molecular, metabolic, and immune features associated with oxidative phosphorylation in melanoma brain metastases. *Neurooncol Adv.* 2021;3(1):vdaa177.
15. Krepler C, Sproesser K, Brafford P, et al. A comprehensive patient-derived xenograft collection representing the heterogeneity of melanoma. *Cell Rep.* 2017;21(7):1953–1967.
16. Boire A, Brastianos PK, Garzia L, Valiente M. Brain metastasis. *Nat Rev Cancer.* 2020;20(1):4–11.
17. Varaljai R, Horn S, Sucker A, et al. Integrative genomic analyses of patient-matched intracranial and extracranial metastases reveal a novel brain-specific landscape of genetic variants in driver genes of malignant melanoma. *Cancers (Basel).* 2021;13(4):1–15.
18. Chen G, Chakravarti N, Aardalen K, et al. Molecular profiling of patient-matched brain and extracranial melanoma metastases implicates the PI3K pathway as a therapeutic target. *Clin Cancer Res.* 2014;20(21):5537–5546.
19. Rabbie R, Ferguson P, Wong K, et al. The mutational landscape of melanoma brain metastases presenting as the first visceral site of recurrence. *Br J Cancer.* 2021;124(1):156–160.
20. Eroglu Z, Holmen SL, Chen Q, et al. Melanoma central nervous system metastases: an update to approaches, challenges, and opportunities. *Pigment Cell Melanoma Res.* 2019;32(3):458–469.
21. Davies MA, Stemke-Hale K, Lin E, et al. Integrated molecular and clinical analysis of AKT activation in metastatic melanoma. *Clin Cancer Res.* 2009;15(24):7538–7546.
22. Niessner H, Schmitz J, Tabatabai G, et al. PI3K pathway inhibition achieves potent antitumor activity in melanoma brain metastases in vitro and in vivo. *Clin Cancer Res.* 2016;22(23):5818–5828.
23. Kircher DA, Trombetti KA, Silvis MR, et al. AKT1(E17K) activates focal adhesion kinase and promotes melanoma brain metastasis. *Mol Cancer Res.* 2019;17(9):1787–1800.
24. Aizer AA, Lamba N, Ahluwalia MS, et al. Brain metastases: a Society for Neuro-Oncology (SNO) consensus review on current management and future directions. *Neuro Oncol.* 24(10):1613–1646.
25. Garman B, Anastopoulos IN, Krepler C, et al. Genetic and genomic characterization of 462 melanoma patient-derived xenografts, tumor biopsies, and cell lines. *Cell Rep.* 2017;21(7):1936–1952.
26. Akbani R, Ng PK, Werner HM, et al. A pan-cancer proteomic perspective on The Cancer Genome Atlas. *Nat Commun.* 2014;5:1–14.
27. Opazo F, Punge A, Buckers J, et al. Limited intermixing of synaptic vesicle components upon vesicle recycling. *Traffic.* 2010;11(6):800–812.
28. Salvati L, Mandala M, Massi D. Melanoma brain metastases: review of histopathological features and immune-molecular aspects. *Melanoma Manag.* 2020;7(2):MMT44.
29. Xie TX, Huang FJ, Aldape KD, et al. Activation of stat3 in human melanoma promotes brain metastasis. *Cancer Res.* 2006;66(6):3188–3196.
30. Vultur A, Villanueva J, Krepler C, et al. MEK inhibition affects STAT3 signaling and invasion in human melanoma cell lines. *Oncogene.* 2014;33(14):1850–1861.
31. Hodis E, Watson IR, Kryukov GV, et al. A landscape of driver mutations in melanoma. *Cell.* 2012;150(2):251–263.
32. van Leeuwen FN, van Delft S, Kain HE, van der Kammen RA, Collard JG. Rac regulates phosphorylation of the myosin-II heavy chain, actinomyosin disassembly and cell spreading. *Nat Cell Biol.* 1999;1(4):242–248.
33. Deshmukh J, Pofahl R, Haase I. Epidermal Rac1 regulates the DNA damage response and protects from UV-light-induced keratinocyte apoptosis and skin carcinogenesis. *Cell Death Dis.* 2017;8(3):e2664.
34. Cannon AC, Uribe-Alvarez C, Chernoff J. RAC1 as a Therapeutic target in malignant melanoma. *Trends Cancer.* 2020;6(6):478–488.
35. Chauhan BK, Lou M, Zheng Y, Lang RA. Balanced Rac1 and RhoA activities regulate cell shape and drive invagination morphogenesis in epithelia. *Proc Natl Acad Sci USA.* 2011;108(45):18289–18294.
36. Byrne KM, Monsefi N, Dawson JC, et al. Bistability in the Rac1, PAK, and RhoA signaling network drives actin cytoskeleton dynamics and cell motility switches. *Cell Syst.* 2016;2(1):38–48.
37. Senger DL, Tudan C, Guiot MC, et al. Suppression of Rac activity induces apoptosis of human glioma cells but not normal human astrocytes. *Cancer Res.* 2002;62(7):2131–2140.
38. Lu H, Liu S, Zhang G, et al. PAK signalling drives acquired drug resistance to MAPK inhibitors in BRAF-mutant melanomas. *Nature.* 2017;550(7674):133–136.
39. de Curtis I. Roles of Rac1 and Rac3 GTPases during the development of cortical and hippocampal GABAergic interneurons. *Front Cell Neurosci.* 2014;8:307.
40. Saci A, Cantley LC, Carpenter CL. Rac1 regulates the activity of mTORC1 and mTORC2 and controls cellular size. *Mol Cell.* 2011;42(1):50–61.
41. Broman KK, Dossett LA, Sun J, Eroglu Z, Zager JS. Update on BRAF and MEK inhibition for treatment of melanoma in metastatic, unresectable, and adjuvant settings. *Expert Opin Drug Saf.* 2019;18(5):381–392.
42. Sanchez-Alegria K, Flores-Leon M, Avila-Munoz E, Rodriguez-Corona N, Arias C. PI3K signaling in neurons: a central node for the control of multiple functions. *Int J Mol Sci .* 2018;19(12):1–15.
43. Ferro E, Goitre L, Retta SF, Trabalzini L. The Interplay between ROS and Ras GTPases: physiological and pathological implications. *J Signal Transduct.* 2012;2012:365769.
44. Chin L, Garraway LA, Fisher DE. Malignant melanoma: genetics and therapeutics in the genomic era. *Genes Dev.* 2006;20(16):2149–2182.
45. Watson IR, Li L, Cabeceiras PK, et al. The RAC1 P29S hotspot mutation in melanoma confers resistance to pharmacological inhibition of RAF. *Cancer Res.* 2014;74(17):4845–4852.
46. Govek EE, Newey SE, Van Aelst L. The role of the Rho GTPases in neuronal development. *Genes Dev.* 2005;19(1):1–49.
47. Jacobs T, Causeret F, Nishimura YV, et al. Localized activation of p21-activated kinase controls neuronal polarity and morphology. *J Neurosci.* 2007;27(32):8604–8615.
48. Ham J, Eilers A, Whitfield J, Neame SJ, Shah B. c-Jun and the transcriptional control of neuronal apoptosis. *Biochem Pharmacol.* 2000;60(8):1015–1021.
49. Fukumura K, Malgulwar PB, Fischer GM, et al. Multi-omic molecular profiling reveals potentially targetable abnormalities shared across multiple histologies of brain metastasis. *Acta Neuropathol.* 2021;141(2):303–321.
50. Derakhshan F, Toth C. Insulin and the brain. *Curr Diabetes Rev.* 2013;9(2):102–116.